Lifetime design, operation, and cost analysis for the energy system of a retrofitted cargo vessel with fuel cells and batteries

Mylonopoulos, Foivos; Durgaprasad, Sankarshan; Coraddu, Andrea; Polinder, Henk

DOI
10.1016/j.ijhydene.2024.10.235

Publication date
2024

Document Version
Final published version

Published in
International Journal of Hydrogen Energy

International Journal of Hydrogen Energy 91 (2024) 1262–1273

Contents lists available at ScienceDirect

International Journal of Hydrogen Energy

journal homepage: www.elsevier.com/locate/he

Lifetime design, operation, and cost analysis for the energy system of a retrofitted cargo vessel with fuel cells and batteries

Foivos Mylonopoulos *, Sankarshan Durgaprasad, Andrea Coraddu, Henk Polinder

Department of Maritime and Transport Technology, Delft University of Technology, 2628, CD Delft, the Netherlands

ARTICLE INFO

Keywords:
Lifetime
Fuel cell
Battery
Design
Operation
Cost

ABSTRACT

Fuel cell-battery electric drivetrains are attractive alternatives to reduce the shipping emissions. This research focuses on emission-free cargo vessels and provides insight on the design, lifetime operation and costs of hydrogen-hybrid systems, which require further research for increased utilization. A representative round trip is created by analysing one-year operational data, based on load ramps and power frequency. A low-pass filter controller is employed for power distribution. For the lifetime cost analysis, 14 scenarios with varying capital and operational expenses were considered. The Net Present Value of the retrofitted fuel cell-battery propulsion system can be up to $ 2.2 million lower or up to $ 18.8 million higher than the original diesel mechanical configuration, highly dependent on the costs of green hydrogen and carbon taxes. The main propulsion system weights and volumes of the two versions are comparable, but the hydrogen tank (68 tons, 193 m^3) poses significant design and safety challenges.

1. Introduction

Approximately 90% of the world's goods are transported by marine vessels, most of which are powered by diesel engines, which emit harmful exhaust gases such as carbon dioxide (CO_2) and monoxide [1]. The shipping industry is responsible for 3% of global emissions but this percentage may increase exponentially in the next few years without drastic changes in the utilized fuels and power systems of ships [2]. Cargo vessels including bulk carriers, containerships and oil tankers represent 85–90% of the world's merchant fleet according to Ref. [3]. General cargo vessels are a subcategory of merchant ships and they are usually short sea vessels operating between countries in proximity to urban areas. Hence, reducing the carbon footprint of such ships is crucial.

The International Maritime Organization (IMO) envisages a 40% reduction in carbon emissions by 2030 (compared to 2008) and until this period the goal is to cover 5–10% of the required global shipping energy by alternative fuels (e.g., hydrogen, methanol, ammonia) and power sources (e.g., fuel cells, batteries, solar panels, wind turbines) [4]. The emissions should be reduced by 70–80% until 2040, and the ultimate maritime goal is to reach net-zero well-to-wake emissions by 2050. The adoption and increasing utilization of green fuels and systems will be crucial to adhere to the strict regulatory requirements and achieve the maritime emission targets.

Hydrogen fuel cells and lithium-ion batteries are among the most attractive zero-emission alternatives to conventional diesel propulsion systems for short sea cargo vessels [5,6]. Fuel cells and batteries have low energy density, so they can be used for ships with short sailing distances near refuelling and recharging infrastructures. Despite the safety concerns associated with the explosiveness of hydrogen and the fire risks of batteries, there has been an increasing interest in these new technologies as these hazards can be mitigated by implementing appropriate risk control options [7]. Hybrid configurations with fuel cells and batteries as power supply sources eliminate the dynamic limitations of pure hydrogen-based systems and the weight limitations of pure battery-electric propulsion [6].

Different studies have focused on the design and operation of hybrid ship energy systems. A comprehensive review on modelling and optimization of the power and propulsion components is presented in Ref. [8]. The focus of this literature review section is on the design and operation of ship power systems that utilize alternative energy sources, with a particular emphasis on fuel cells and batteries.

Ganjian et al. [9] presented an optimal design analysis for a fuel cell-battery hybrid fishing vessel to minimize system mass, volume, costs and improve electrical safety. A genetic algorithm was used to optimize separately each objective function. The degradation and the

* Corresponding author.
E-mail address: F.P.Mylonopoulos@tudelft.nl (F. Mylonopoulos).

https://doi.org/10.1016/j.ijhydene.2024.10.235
Received 13 May 2024; Received in revised form 2 September 2024; Accepted 16 October 2024
Available online 21 October 2024

replacement costs of the components were not included in the optimization analysis. Vieira et al. [10] optimized the configuration of a hybrid platform supply vessel with fuel cells, diesel gensets and batteries to reduce the CO_2 emissions. However, the total costs were not included in the analysis. Wang et al. [11] proposed a nested design and control optimization for a similar type of hybrid system with [10], but including the capital and operational costs in the objective functions. The degradation of batteries and fuel cells was not included in the two studies [10,11]. Wu and Bucknall [12] presented a two-layer optimization for a fuel cell-battery driven ferry incorporating the degradation effects, for an averaged simplified load profile. The focus of this study was on the estimation of emissions reduction after retrofitting. Bassam et al. [13] developed an improved Proportional Integral (PI) controller to reduce the fuel cell consumption and degradation. The controller was tuned to satisfy the specific input conditions of the given power profile. The same authors in Ref. [14] developed a multi-scheme control strategy that could switch between different energy management approaches during the a-priori predicted power profile, based on battery SoC and power demand. However, the online adjustment of control strategies due to unpredicted operating conditions was not demonstrated.

The above studies [9–14] focus on global optimization and do not include real-time controllers. Some research works that utilize online control approaches are listed below.

In [15,16] fuzzy logic controllers were used to optimize fuel cell-driven ships with hybrid energy storage systems, in terms of efficiency and components' degradation. The implemented strategies are rule-based, so they rely on human experience and engineering knowledge. Si et al. [17] also implemented fuzzy rules, but combined with an artificial bee colony algorithm to optimize the design of a bulk carrier consisting of wind turbines, solar panels, fuel cells, batteries and diesel gensets. The practical challenges of integrating all these systems into one design were not discussed. Fan et al. [18] presented a robustly coordinated two-stage control approach for the power splitting between fuel cells, batteries and diesel gensets. Pre- and intra-voyage information (based on short term prediction) were utilized to reduce the operational costs and emissions.

The above studies [9–18] include optimization problems which do not take into account the design, lifetime performance and cost uncertainties of retrofitting. The remainder of the literature section focuses on studies that consider the systems' (fuel cells and batteries) lifecycle performance and/or costs.

Zhu et al. [19] optimized a diesel-battery hybrid ship system using a genetic algorithm and a rule-based controller to minimize the annual fuel consumption, emissions, and lifecycle costs, considering a single power profile. The diesel tank and converter investment costs, and the maintenance costs of the components were not considered. Furthermore, there was no degradation model for the estimation of battery lifetime and its replacement cost. A battery cycling degradation model was presented by Chen et al. [20] for the minimization of lifecycle costs of a diesel genset-battery hybrid passenger vessel. The genset model equations, the battery calendar aging effects and the fuel prices were not discussed. Wang et al. [21] presented a lifecycle optimization problem for a battery hybrid energy storage system, considering the design cost and lifetime of batteries and supercapacitors. However, the investment costs of other systems such as engines, converters, tanks, motors, and the fuel and maintenance costs were not considered in the economic analysis.

Bassam et al. [22] optimized the sizes of a hydrogen-hybrid ferry using a PI controller considering Capital Expenses (CAPEX), Operational Expenses (OPEX), maintenance and replacement costs. There were no battery and fuel cell degradation models. The components were replaced at their expected end of life, provided by the manufacturer. The implemented PI controller is not real-time, so it cannot adapt to varying operating conditions due to uncertainties and disturbances. Its parameters have been tuned to satisfy the specific conditions of a given power profile. Dall'armi et al. [23] used the Mixed Integer Linear Programming algorithm, for the optimal sizing problem, to minimize the fuel consumption and degradation, focusing on the lifetime performance and the progressive ageing of fuel cells and batteries. Fixed fuel and component prices were considered for the cost analysis. Dall'armi et al. [24] extended the previous work [23] by utilizing the MonteCarlo analysis to account for uncertainties related to hydrogen, fuel cell and battery costs. In both studies [23,24] a single power profile was used as input to the optimization frameworks. The original and the retrofitted versions were not compared in terms of design, lifetime operation and costs. Moreover, these are global optimization studies in which the operating profiles are assumed to be known in advance, without real-time controller capabilities. Zhang et al. [25] developed an online real-time controller combining the Equivalent Consumption Minimization Strategy (ECMS) and a filter-based approach to maximize the power plant efficiency and minimize the fuel cell and battery degradation of a passenger ship. Chen et al. [26] optimized the size and control of a fuel cell-battery-supercapacitor hybrid system, using a controller combining support vector machine and low-pass filter, to minimize energy losses, bus voltage fluctuations and battery degradation. In both studies [25,26], the impact of the design and control solutions on the lifetime costs were not discussed, since the focus was on the technical objectives.

Lagemann et al. [27] presented a study for the selection of the optimal power systems and fuels in terms of lifecycle costs and emissions, considering the potential retrofits along the lifetime of the case vessel. Methanol, ammonia, hydrogen and liquefied natural gas were among the fuels that were compared, but hybrid configurations were not considered due to the constraint that the algorithm can select only one compatible fuel and power system option. Uncertainties in fuel costs and carbon emission prices were included in the authors' extended work in Ref. [28]. In both studies [27,28], a high-level approach was used for the system design and operation. There was no discussion about the configurations and the control of the systems that can have a significant impact on the estimation of the lifetime costs.

There have been a few studies that focus on the techno-economic feasibility and lifecycle assessment of fuel cell and battery powered vessels.

Monaaf et al. [29] presented a lifetime techno-economic study for a retrofitted fully battery powered ferry. The packs were sized based on the Depth of Discharge (DoD) and the maximum load. The calendar aging effects were not considered, and the cycling degradation was estimated assuming the battery operates at 80% DoD over its lifetime, for a single profile. Furthermore, the retrofitting implications in terms of overall weight and volume changes were not discussed. Wang et al. [30] presented a lifecycle emission and cost assessment for two ferries, a tug and a trawler, that were conceptually retrofitted with hydrogen engines. This study did not discuss the uncertainties associated with the low technological system maturity, the required retrofitting changes, and the design and cost specifications of the rest of the energy systems.

Inal et al. [31] presented a lifecycle emission and cost assessment case study for a retrofitted hydrogen-fuelled general cargo vessel, and compared the results to the original diesel version. The tank placement onboard and the replacement of the fuel cell stacks were not considered. It was assumed that the fuel cells can last for 15 years and cover the load fluctuations without hybridization with batteries. Furthermore, fixed fuel and component prices were considered for the economic analysis. Karvounis et al. [32] presented a lifecycle emission and cost assessment using hydrogen and ammonia as substitute fuels for marine engines, but without discussing the practicality and feasibility of retrofitting considering the design constraints (weight, volume, costs) and the low system technical maturity. In both case studies of short sea cargo vessels [31,32] a single power profile was considered. Trillos et al. [33] demonstrated that a fuel cell-battery passenger ferry could reduce the well-to-wake emissions by 89% compared to the diesel-hybrid version. This study focused on environmental and health aspects such as emissions, maritime ecotoxicity and human carcinogenic toxicity. The impact of the design decisions on the lifetime costs was not discussed.

Overall, the studies that perform a lifecycle emission and cost assessment do not discuss the control strategies and lifetime operation of the systems.

The main outcomes and gaps from the literature review are summarized below.

- There is a gap in the literature for retrofitting studies of cargo vessels with hydrogen fuel cells and batteries, considering the impact of multiple power profiles on system sizing and control, using a robust real-time controller. Most studies focus on developing control approaches and sizing methods tailored to specific applications with a single (simplified) power profile.
- There is a lack of comprehensive design, lifetime operation and cost analyses under varying economic scenarios, especially for hydrogen-based ship energy systems.
- To the best of the authors' knowledge, there is no study that considers all the following: the degradation effects of both fuel cells and batteries (combined cycling and calendar aging), the replacement periods and costs, and the tank sizing based on the lifetime increase in fuel consumption.

The focus of this research is on the design and operation of emission-free cargo ships. A diesel-mechanical vessel is retrofitted with hydrogen fuel cells and lithium-ion batteries to reduce its environmental footprint. A representative round trip is selected for the analysis. The power distribution between the fuel cells and batteries, and the system sizes are obtained using a real-time low-pass filter controller. The fuel consumption, system weights and volumes, component degradations, and lifetime costs of the retrofitted fuel cell-battery propulsion system are estimated and compared to the conventional diesel mechanical version. This study provides insight on the design and operation of hydrogen hybrid cargo vessels, for the research community, shipowners and vessel operators regarding the implications and uncertainties of such retrofitting.

To summarize, the novelty of this study is threefold.

- Proposal of a method for the selection of representative ship power profiles.
- A detailed methodology including system design, sizing, real-time control, lifecycle operation, and net present value analysis of a ship propulsion system for varying OPEX and CAPEX.
- Estimation of fuel cell degradation, combined battery cycling and calendar aging, component replacement costs, and the impact of degradation on tank sizing.

The rest of the paper is organised as follows. In Section 2, the case study details for the vessel and the retrofitted hydrogen-based energy system are presented. In Section 3, the proposed methodology for the design, operation and cost analysis is described. The results from the analysis and the simulations are discussed in Section 4. Finally, the concluding remarks are presented in Section 5.

2. Case study

In this section, the case vessel details and the retrofitted hydrogen-based energy system characteristics are discussed.

2.1. Vessel details

The case ship is a diesel mechanical general cargo ship 90 m long, 12.5 m wide and it carries 3638 tons of cargo [34]. It is retrofitted with hydrogen fuel cells and batteries as the power supply components to minimize the onboard emissions. The vessel does not have a fixed load profile and schedule since it sails between different countries, mainly in the Baltic and the North Sea.

2.2. System design for the retrofitted version

The configuration of the system for the retrofitted hydrogen-based propulsion system is shown in Fig. 1.

The original version has a direct-drive diesel mechanical system with a main engine of 1.8 MW (oversized system), and a controllable pitch propeller. In the new hydrogen-based version (Fig. 1), the engine is replaced by two AC variable speed electric motors on the same shaft, connected to a fixed pitch propeller. The number and types of fuel cells and batteries will be determined after employing the real-time control strategy, which will be discussed in Section 3.2. In the new hybrid configuration, there are two DC buses for redundancy in case of failure to ensure that propulsive power is available under different off-design conditions. From a practical perspective, after discussions with the vessel operators, it is recommended to install an emergency/standby diesel generator (800 kW), that will be used in case hydrogen is not available at the right place or quantity. The original and the retrofitted design will be discussed in more detail in Section 4.5.

3. Methodology

A flowchart of the methodology proposed in this study for the design, operation, and cost analysis is shown in Fig. 2.

In Step 1, the power profiles of the vessel, considering one-year operational data, are analyzed in terms of load ramps and power frequency distribution, to select a representative round trip. Then in Step 2, the fuel cells are sized based on the maximum power demand of the vessel. In Step 3, a real-time low-pass filter based control strategy is implemented to distribute the power between the components. The batteries are iteratively sized until the power balance and SoC constraints are satisfied for all the profiles of the round trip. The obtained fuel cell and battery power distributions are used as input to calculate the degradation of the components in Steps 4 and 5. Finally, in Step 6, the lifetime system costs are estimated following a sensitivity analysis for varying operational and capital costs. The retrofitted energy system is compared to the original configuration in terms of design and lifetime costs.

The methodology is explained in detail in Sections 3.1-3.5.

The following assumptions are considered in this study.

- Only the propulsive power demand of the vessel is considered, with a sampling interval of 5 min, without any auxiliary loads and systems such as filters, cooling, and safety equipment.
- For the cost analysis, it is assumed that the hydrogen-based version is refuelled with green hydrogen that is always available. This is an optimistic assumption since there are certain challenges that need to

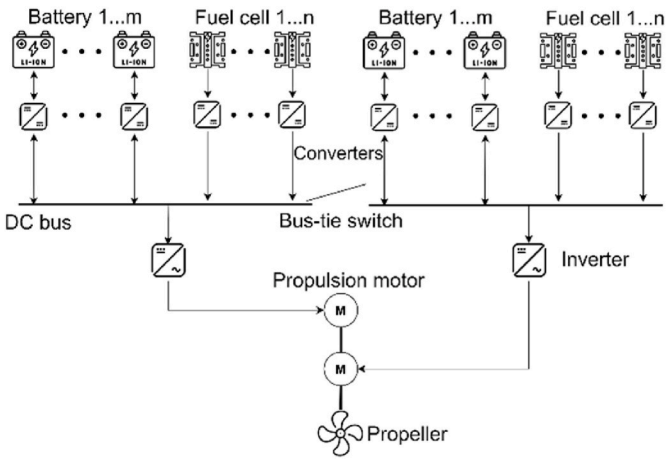

Fig. 1. Retrofitted energy system.

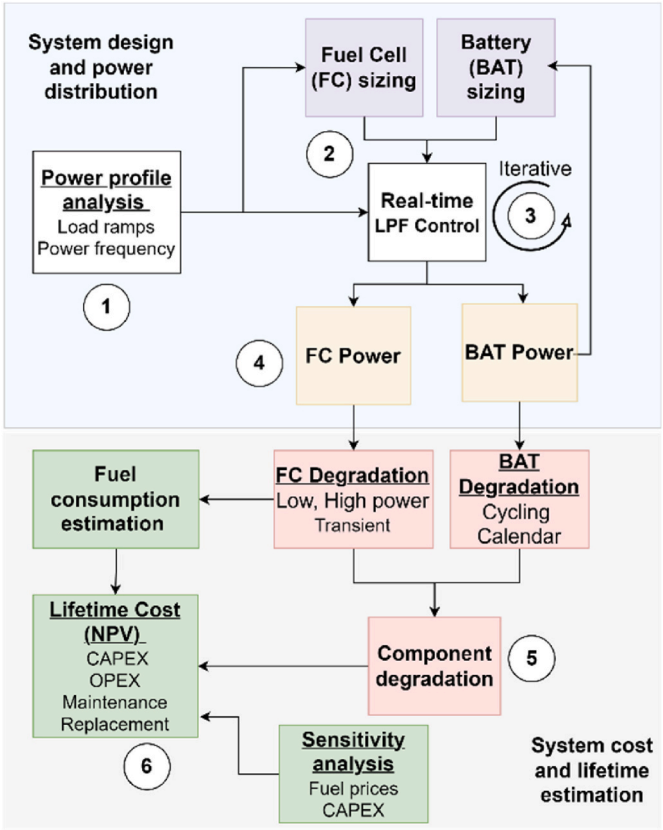

Fig. 2. Flowchart for the design, operation and cost analysis.

be addressed for wide availability of green hydrogen such as: high production cost and limited existing infrastructure including storage systems, distribution and transportation networks. The stringent environmental regulations, and the price drop and development of renewable systems (e.g., wind and solar) are expected to enhance the economics of green hydrogen production in the future [35]. Regarding the fuel storage equipment, various methods such as salt caverns and hydrogen carriers are investigated to store large amounts of fuel [35]. The produced green hydrogen may be in remote locations or far away from the ship, so there might be a need for a large pipeline network or intermodal fuel tank transportation (e.g., trucks, trains) as part of the supply chain network [36].

- The vessel, after retrofitting, has a remaining lifetime of 20 years, and it operates in the same round trip.
- Only the fuel cells and the batteries require replacement during the 20-year period.
- The recycling of the components and their residual cost values at the end of the vessel's lifetime are not considered.

3.1. Analysis of power profiles

All the power profiles (one-year data) of the case vessel are analyzed in terms of frequency of power and load ramps. Compared to the one-year data, the representative round trip is selected such that the vessel operates for a similar percentage of the sample data at the same power ranges (e.g., 100–200 kW, 500–600 kW) and has a similar percentage of fluctuations at various load ramps (e.g., 5–10% ΔkW/Δt). A few profiles were chosen for the round trip to reduce the computational burden, but they still have an accurate representation of actual ship voyages. The power distribution is an important key performance indicator for more accurate lifetime fuel consumption estimation, and the load ramps are critical for the estimation of fuel cell degradation.

The selected round trip should include the most power demanding operating conditions for fuel cell sizing, the most energy intensive fluctuations for battery sizing, and the longest profile with the highest fuel consumption for tank sizing.

3.2. Real-time low-pass filter-based controller

The case vessel does not have a fixed power profile and schedule, so a robustly coordinated real-time control strategy that can be implemented to different power profiles is necessary. Fuzzy-logic rule-based approaches can be simple and effective but they rely on human expertise, and according to Ref. [25] they can be highly dependent on specific power profiles and operating conditions, so they are not selected for this study. Some possible real-time control approaches that can be used are: ECMS, Model Predictive Control (MPC), or Artificial Intelligent (AI) methods. The studies that use ECMS usually focus on fuel consumption minimization, neglecting other objectives such as the degradation of components [25]. Moreover, the controller might face challenges adapting to unpredictable sailing profiles due to incorrect real-time tuning of the equivalence factors. MPC approaches can be used in dynamic simulations to predict future states and optimize the system's operation at every time step, but they usually require high fidelity models and significant computational time. Furthermore, the creation of a robust controller can be challenging due to the disturbances and uncertainties [37]. AI methods can also be used to predict future operating states but they may require a large amount of data and resources to produce accurate, physically-consistent and interpretable results [8]. Predictive methods can be beneficial in scenarios where significant battery charging and discharging is required (e.g., peak shaving functions), as they enable prior charging to ensure the power and energy demand constraints are satisfied.

In this study, a filter-based control approach is selected due to its simplicity in terms of implementation, robustness under different operating conditions, and low computational complexity. The developed low-pass filter-based real-time controller for operation is shown in Fig. 3.

The generic fuel cell, battery, and converter models from Simulink are used for the analysis. The DC bus voltage is controlled by a PI controller at 1000 V. The low-frequency current is delivered by the fuel cells and the high-frequency current by the batteries. The lower the time constant in the low-pass filter, the faster the fuel cells respond to load changes and thus degrade. The battery SoC is also controlled around 50% with a P controller to reduce its degradation. The saturation blocks are used to ensure that the current limits for the components are not exceeded. Overall, this low-pass filter control approach provides at low complexity and computational requirements: real-time operation for different power profiles, controllability of fuel cell and battery operation for reduced fuel consumption or components' degradation, and stable DC bus system voltage. More details about the models and the control strategy are discussed in the authors' previous work [34].

The battery power is estimated by subtracting the fuel cell power from the load demand. The energy capacity is estimated considering a C-rate equal to 1. For each profile of the round trip, the power supplied by

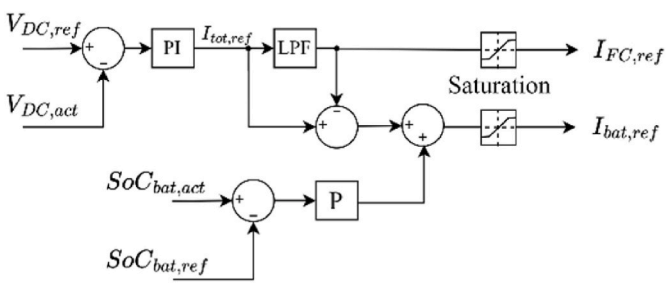

Fig. 3. Real-time low-pass filter controller.

the fuel cells and the batteries should be equal to the load demand at each time step, and the battery SoC should remain between 20 and 80% for the selected low pass filter time constant. If one of the conditions is not satisfied, the battery size should be modified. Then, the battery components can be selected, and the fuel consumption for one round trip can be calculated using the Simulink model, as presented in Ref. [34], for the considered fuel cell stacks [38].

In the proposed control strategy, the battery is used for smoothing the load experienced by the fuel cells and for providing ramp support. For such battery functions, it can be simple and effective to use a low-pass filter control strategy [25,26].

3.3. Degradation of fuel cells and batteries

Fuel cell degradation at chemical scale may affect different parts such as the membrane and the electrodes. The reactant humidity, temperature, stoichiometry and flow rates are critical operating factors for the efficiency and durability of the fuel cell stacks. Low relative humidity or high temperature can lead to structural dissolution of the membrane [39]. Low reactants' flow rates and low relative humidity may lead to the formation of radicals which can cause platinum dissolution and carbon support corrosion in the catalyst layer. Those lead to impedance rise and thus voltage decay for the cells [39]. The carbon support corrosion can also lead to active surface area loss (for reactions) or conductivity loss which also result in voltage drop.

The focus of this study is on the degradation of fuel cells based on their operating power levels. It is defined as the voltage drop of a single cell at constant current output, assuming that the reduction of voltage is the same across all the cells of each stack [23,24].

The total degradation is measured in microvolts (μV), and it is a summation of the voltage drops due to transient loading, start/stop cycles, low power operation (<10% P_{max}), and high-power operation (>90% P_{max}), where P_{max} is the rated power of the fuel cell stacks [40].

The degradation of the fuel cells is described by Equations (1)–(5). It is assumed that all the fuel cells operate at the same power level and there is no individual control and switch on/off during manoeuvring and cruising phases.

$$dv_{ramp}(t+1) = |P_{FC}(t) - P_{FC}(t+1)| \bullet \Delta v_{ramp} \tag{1}$$

$$dv_{start}(t) = \delta_{start}(t) \bullet \Delta v_{start} \tag{2}$$

$$dv_{low}(t) = \begin{cases} a_{low} \bullet \frac{0.1P_{max} - P_{FC}}{P_{max}} \bullet \Delta t, if\ P_{FC} < 0.1P_{max} \\ 0, otherwise \end{cases} \tag{3}$$

$$dv_{high}(t) = \begin{cases} a_{high} \bullet \frac{P_{FC} - 0.9P_{max}}{0.1P_{max}} \bullet \Delta t, if\ P_{FC} > 0.9P_{max} \\ 0, otherwise \end{cases} \tag{4}$$

$$dv_{total}(t) = dv_{ramp}(t) + dv_{start}(t) + dv_{low}(t) + dv_{high}(t)\ (\mu V) \tag{5}$$

where $dv_{ramp}(t)$ is the voltage reduction due to the load variations, and it is proportional to the constant transient coefficient Δv_{ramp}. In Equation (2), $dV_{start}(t)$ expresses the voltage reduction due to startup of the fuel cell stack, and it is proportional to the constant start/stop coefficient ΔV_{start}. The binary variable $\delta_{start}(t)$ is either 0 or 1, if the fuel cell is switched off or on respectively. In this study, it is assumed that the fuel cells are always switched on during the voyage. In Equations (3) and (4), the degradation due to low power and high-power operation is expressed. The values for the parameters of fuel cell degradation are shown in Table 1.

The batteries degrade due to cycling and calendar aging.

The critical lithium-ion battery aging factors are the DoD, temperature and C-rate. High DoD can lead to structural disordering and thus loss of active material or lithium inventory which lead to cell capacity drop [39]. The temperature effect is considered only for calendar aging in this study. High temperatures can lead to binder decomposition and contact loss in the anode side. These can cause conductivity loss and impedance rise, leading to power or capacity fade [39]. The effect of C-rate on battery degradation is not analyzed in this study. However, high C-rates can lead to particle cracking, lithium plating or structural disordering [39].

Table 1
Values for fuel cell degradation parameters.

Parameter	Value/Unit
Δv_{ramp}	0.4185 μV/ ΔkW [41]
ΔV_{start}	23.91 μV/ cycle [23]
a_{low}	10.17 μV/ hour [42]
a_{high}	11.74 μV/ hour [42]

For cycling aging, the rainflow counting algorithm was used to estimate the number of cycles, for each profile, at a specific DoD [43]. The Equivalent Cycles (EC) are calculated as shown in Equation (6).

$$EC = \sum_{j}^{n} \left(cycle\ range_j \bullet cycle\ number_j\right) / DoD \tag{6}$$

where j is each measured half-cycle or full cycle. The cycle range (SoC range) is multiplied by the cycles' number for each measured half or full cycle obtained from the rainflow counting algorithm. The DoD is the difference between the maximum and minimum SoC for each profile. The capacity loss due to cycling aging is defined as a percentage from the ratio between the measured equivalent cycles over the maximum number of cycles at the specific DoD, based on the datasheet of the battery [44]. A calendar aging prediction model was developed by Ali et al. [45], as shown in Equation (7), to estimate the battery degradation when it is not operated, depending on the storage temperature, SoC, and idling time.

$$Idling\ Degradation = a_1 e^{a_2 SoC} \bullet b_1 e^{\frac{b_2}{T}} \bullet t^{c_1} \tag{7}$$

where a_1, a_2, b_1, b_2 and c_1 are the fitting parameters of lithium-ion batteries. These parameters have been obtained from experiments for different chemistries [45]. In this study, lithium iron phosphate (LFP) batteries are used. The SoC ranges from 0 to 1, T is the storage temperature in Kelvin and t is the time that the battery is stored in days. The LFP battery is stored at 50% SoC and 25 °C, for 36 days at the end of each year when the vessel is not in operation.

3.4. Lifecycle costs of the energy systems

The Net Present Value (NPV) includes the CAPEX and the OPEX, and considers the 20 years of the remaining vessel's lifetime. It is calculated as shown in Equation (8) for both versions (diesel, hydrogen). A sensitivity analysis is performed for varying fuel prices, carbon taxes, and CAPEX of fuel cells and batteries.

$$NPV = CAPEX + \sum_{k=1}^{20} \frac{OPEX_k}{(1+r)^k} \tag{8}$$

where k is the number of years, and r is the interest rate which is assumed to be 5% [28,46,47]. The OPEX includes fuel costs, hydrogen liquefaction, carbon tax costs (only for the diesel-based version), maintenance and component replacement costs. The CAPEX includes the initial investment for the propulsion systems and the storage tanks.

3.5. Design and cost comparison with the diesel mechanical version

The retrofitted hydrogen-hybrid version is compared to the original

diesel mechanical system in terms of lifecycle costs and system design, to investigate the implications of the conversion of the propulsion system. The weights and volumes of the components of the two versions are compared. Design recommendations are also provided for the new fuel cell-battery hybrid configuration.

4. Results and discussion

In this section, the results from the analysis and the simulations are presented and discussed.

4.1. Profile analysis results: load ramps and frequency of power

The data of the propulsive power demand of the original diesel mechanical version is analyzed. The selected round trip from the one-year data should have a similar percentage of the same power ranges and load variations (ramps). The results from the power frequency analysis are shown in Table 2 and summarized in Table 3. The sum of the percentages is equal to 100% for each case. As shown in Table 2, the vessel operates 11.9% of the total one-year sample data between 500 and 600 kW, and 13.4% of the samples of the selected round trip at the same power range. In Table 3, the results are summarized, and it is shown that the representative round trip is very similar to the one-year data, considering power ranges of 500 kW.

The load fluctuation results are shown in Table 4. The sum of the percentages is equal to 100% for each case. The ramps cover both positive and negative power changes for each interval. It is shown that the representative round trip is very similar to the one-year data in terms of percentages of load fluctuations. As expected for a general cargo vessel, about 88.5% of the total load changes are in the range of 0–5% ΔkW/Δt, which indicates that most of the time the vessel operates at almost constant power levels with small fluctuations.

The selected round trip is shown in Fig. 4. It consists of 11 single trips, with the vessel sailing between the Netherlands, Finland, Sweden, Lithuania, and Belgium. The ship starts its first voyage from Dordrecht, Netherlands and ends the last voyage, after 47 days, at the same location. After each voyage, the vessel stays at the port for 1–2.5 days, based on the actual data, for hydrogen refuelling and/or cargo operations. It is assumed that there are appropriate risk control options that enable simultaneous bunkering and cargo loading/unloading, if necessary [7]. According to Ref. [48], it takes around 1 h to refill 1 ton of liquefied hydrogen (LH_2) through direct refuelling by trailers. This option can be more cost-effective and flexible than refuelling with fixed bunkering infrastructure, especially at the early stages of operation [48].

4.2. Real-time low-pass filter control strategy results

The maximum required propulsive power of the round trip is 1230 kW (Fig. 4), but an additional 10% margin is considered for uncertainties in power profiles due to extreme wind and wave conditions. Hence, the total installed fuel cell power is 1350 kW, covered by 9 highly efficient and compact fuel cells of 150 kW each [38].

Table 2
Frequency of power (detailed).

Power range (kW)	One-year data	Selected round trip
0–100	0.8%	0.6%
101–200	6.1%	5.5%
201–300	2.1%	2.5%
301–400	2.1%	2.6%
401–500	3.4%	3.2%
501–600	11.9%	13.4%
601–700	16.6%	21.2%
701–800	21.4%	29.7%
801–900	21.2%	9.1%
901–1000	9.5%	6.1%
1001–1100	1.7%	1.0%
1101–1200	2.7%	4.4%
1201–1300	0.5%	0.7%
1301–1400	0.0%	0.0%

Table 3
Frequency of power (summarized).

Power range (kW)	One-year data	Selected round trip
0–500	14.5%	14.3%
501–1000	80.6%	79.5%
1001–1500	4.9%	6.2%

Table 4
Load fluctuations (ramps).

(±) ΔkW/Δt	One-year data	Selected round trip
0–5%	88.5%	88.4%
5–10%	2.9%	2.7%
10–15%	1.5%	1.5%
15–20%	1.1%	1.1%
>20%	6.0%	6.3%

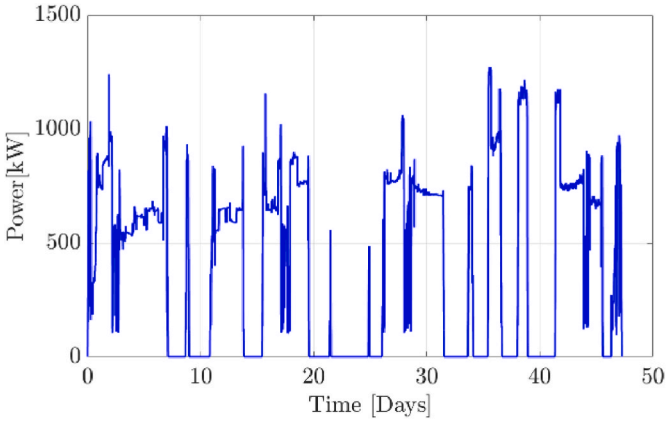

Fig. 4. Selected round trip.

The time constant in the low pass filter is selected such that the fuel cells slowly react to load changes. It is set equal to 10 min, with power measurements of 5 min in the load demand graphs. Hence, the fuel cells slowly follow the power demand for all the profiles, and when fast transients are required, the batteries are used. One profile with a large interval of almost constant power, and one purely manoeuvring profile, with high fluctuations, are shown in Figs. 5a and 6a respectively. The battery SoC is shown in Figs. 5b and 6b respectively for both profiles.

For the constant power profile (Fig. 5), the battery power is close to zero for most of the time during the cruising mode of operation, since there are no significant load fluctuations.

In Fig. 6, for the manoeuvring profile, the battery operates between 25 and 70% SoC, with more fluctuations. At some intervals, the fuel cell power exceeds the load demand since the batteries need to be charged. The P controller (Fig. 3) tries to reduce the gap between the actual SoC and the reference value which is 50%. For all profiles, the SoC at the end of the voyage is equal or greater than 50% (initial value), to avoid shore charging due to safety risks related to fire and explosion, and uncertainties related to infrastructure and electricity availability.

After analysing all 11 profiles of the round trip, the average DoD is equal to 41.3% for the two battery racks of 100 kW, 100 kWh each [44]. Two batteries are installed for active redundancy, and their sizes are selected so that they operate in the recommended SoC range of 30–70% which results in low cycling aging [44]. The power balance and SoC constraints are satisfied for all the profiles of the round trip. The batteries are mainly used for load smoothing and ramp support in all

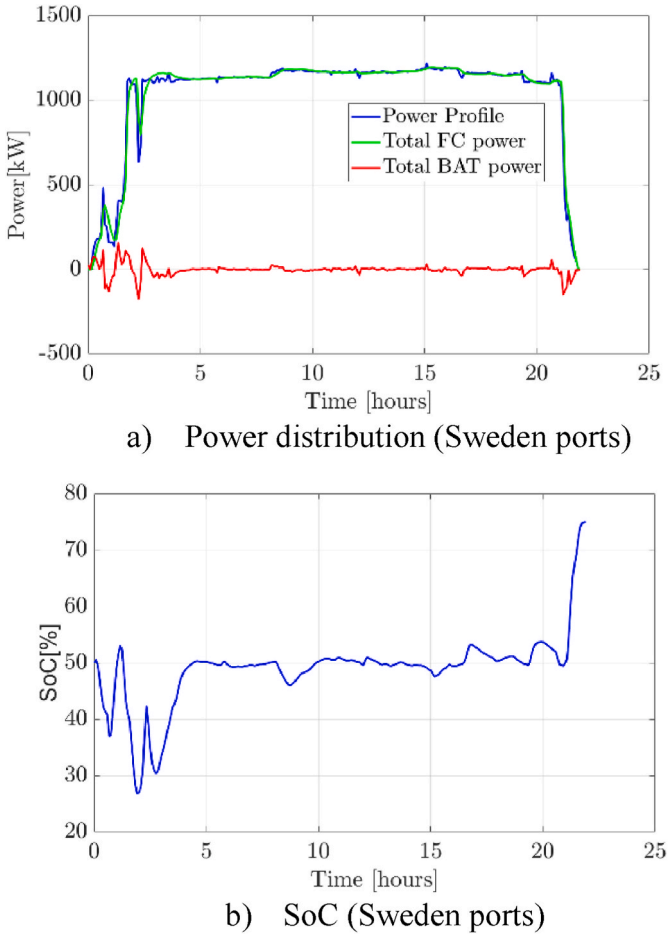

Fig. 5. Constant power profile, a) Power distribution, and b) Battery SoC.

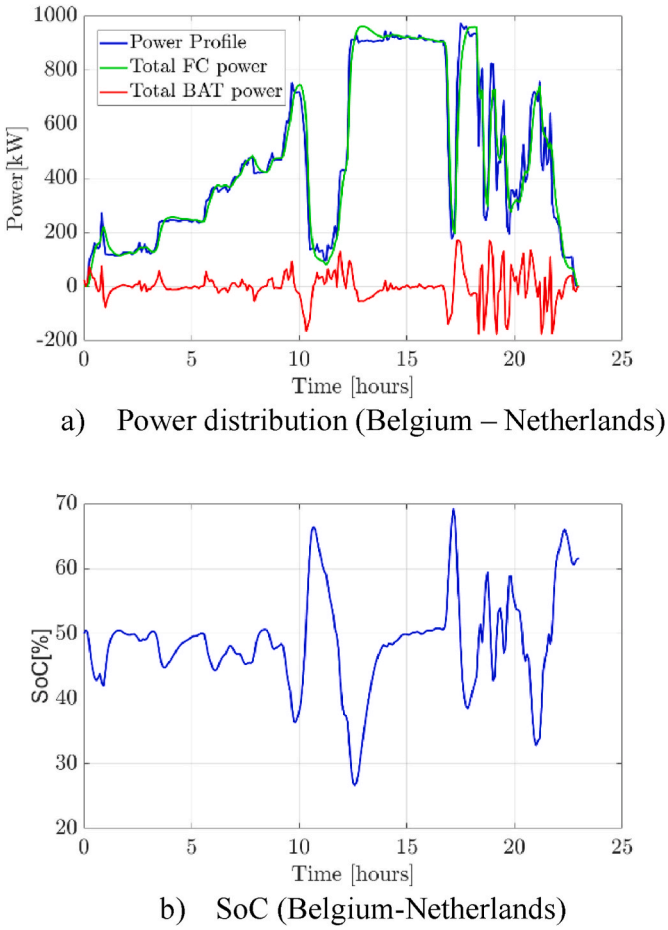

Fig. 6. Manoeuvring power profile, a) Power distribution, and b) Battery SoC.

operating conditions.

To verify the power distribution results of the developed Simulink model and the low-pass filter controller, a simple moving average control strategy, with the same time constant, was developed in MATLAB.

For the moving average controller, the fuel consumption is estimated as shown in Equation (9).

$$F_{FC}(t) = \mathrm{a} \bullet P_{FC}^{2}(t) + b \bullet P_{FC}(t) + c \tag{9}$$

where F_{FC} (t) is the fuel consumption of the fuel cell as a function of time, P_{FC} (t) is the power of the fuel cell as a function of time, and a, b, and c are the quadratic function coefficients based on the actual curve from the manufacturer's datasheet [38].

As a sanity check, the fuel consumption difference between the two models is less than 1% for all the profiles of the round trip.

4.3. Lifetime fuel consumption and degradation of components

The hydrogen consumption is estimated for each voyage of the round trip based on Equation (9). The journey from Dordrecht (Netherlands) to Finland is the longest in duration (170 h) and it requires the largest amount of hydrogen onboard (5.6 tons). This power profile will determine the required size of the LH_2 tank, but an increased consumption due to fuel cell degradation by the end of life of the components, and an additional margin of 15% for spare capacity due to hull fouling, need to be considered [49].

The State of Health (SoH) of the components is estimated based on [23], considering the cumulative voltage drop of the fuel cells and the capacity loss of the batteries. The cell voltage drop is calculated based on Equation (5), and when it is reduced by 15% from a reference value of 0.95 V, the stack needs to be replaced [23]. The maximum fuel cell power at the beginning of life is 175 kW, and the rated power is 150 kW, which corresponds to the end-of-life condition of the stack [23]. Similarly, the battery is replaced when the capacity is reduced by 20% from its maximum value [23,24]. The SoH graph of the components is shown in Fig. 7.

The fuel cells are replaced every 4.92 years or 26,300 operational hours, which is very close to the design life provided by the stack's manufacturer (25,000 h) [38]. The low and high-power fuel cell operating regions are limited, and there are no startup/shutdown cycles during manoeuvring and cruising. The transient loads have the biggest

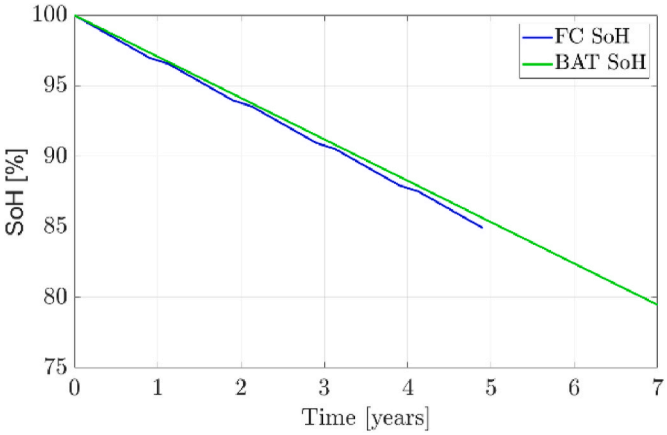

Fig. 7. SoH of fuel cells and batteries.

impact on the total fuel cell degradation. At the end of each year, during the period the vessel is in idle condition, there is no fuel cell degradation. The batteries are replaced every 6.83 years. The annual capacity lost is 2.93% (0.96% due to cycling aging, and 1.97% due to calendar aging).

The progressive increase in hydrogen consumption due to fuel cell degradation (Fig. 8) has been estimated, as a function of voltage drop, based on [23]. After the first round trip, the hydrogen consumption is 24.2 tons, and at the end of life of the fuel cells after 4.9 years, the round trip consumption is 24.5% higher.

To size the hydrogen tank, an additional 15% spare capacity is considered due to various parameters that increase fuel consumption such as hull fouling, boil-off, thermal tank expansion etc. [49]. The LH_2 tank is sized, considering the total margin of 39.5% (24.5 + 15), to contain the 7.8 tons required for the longest voyage with the highest fuel consumption. Hence, considering the gravimetric and volumetric specifications of a cryogenic cylindrical storage tank [48], the LH_2 tank weighs 68 tons, and its volume is 193 m^3.

The fuel consumption of the main propulsion engine in the original diesel-based version was measured with onboard sensors, and the data was provided by the vessel operators. The increase of diesel consumption over time due to the wear and fouling of the main engine parts is shown in Fig. 9. The drops in diesel consumption are due to the periodic maintenance of the engine components, as described in Ref. [50]. It is assumed that the engine can last for 20 years (about 100,000 operating hours), without replacement, for short sea cargo vessels [51].

The Marine Gas Oil (MGO) tank is sized following a similar process with the LH_2 tank. The required volume of the MGO tank is 38 m^3, and it should carry 33.2 tons MGO, considering the longest profile and the required margins.

4.4. *Sensitivity analysis for total lifetime cost estimation of energy systems*

In this subsection, the NPV analysis is presented for varying fuel costs, carbon taxes, and CAPEX of the fuel cells and batteries.

The CAPEX, maintenance and replacement costs for the propulsion systems of the two versions are presented in Table 5. The average cost values are used, when there are two or more references for a specific component, for higher reliability in the prices.

The maintenance costs of the components are uncertain parameters and they have been approximated based on the available literature, since they depend on the way of operation of the systems. It is also assumed for the cost analysis that the efficiency curve of the fuel cell stacks does not improve over time. In a future work, given that more data will be available regarding the long-term operation and further development of fuel cells, the sensitivity analysis can be improved by considering variable maintenance costs and efficiency improvements over time.

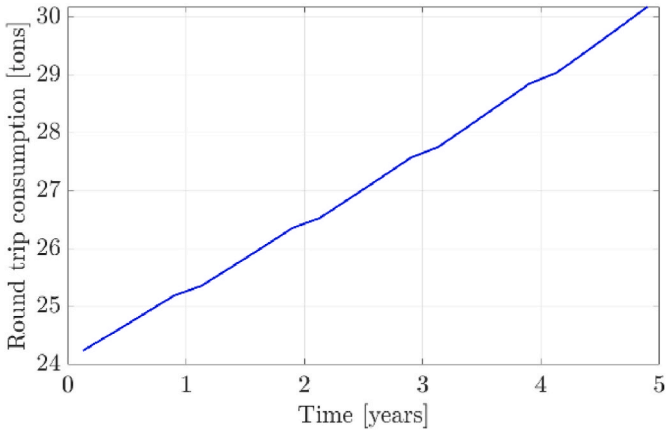

Fig. 8. Hydrogen consumption increase due to fuel cell degradation.

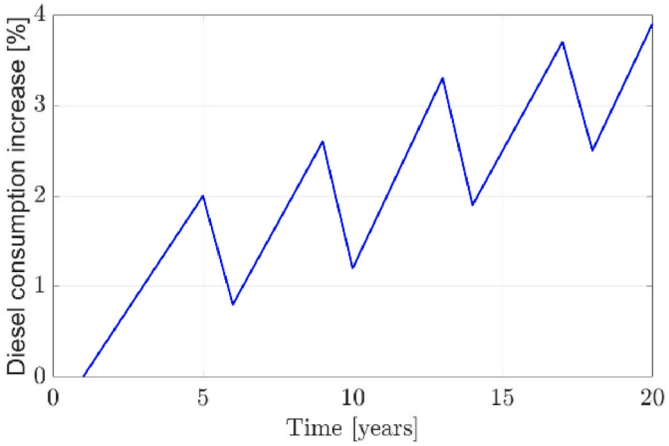

Fig. 9. Diesel consumption increase due to wear and fouling of the main engine parts based on [50].

Table 5
Fixed System costs.

Systems	CAPEX	Maintenance	Replacement
Fuel cell	1014 $/kW [52–56]	1% CAPEX [54]	50% CAPEX [54]
Battery	492 $/kWh [53,57,58]	0.5 $/kW/a [53]	CAPEX *Assumption*
Converter	216 $/kW [46,49,53]	2.6 $/kW/a [46,53]	Not replaced [49]
Motor	133.5 $/kW [46,53]	1.3 $/kW/a [46]	Not replaced [49]
LH_2 tank	233 $/kg H_2 [22,59,60]	Not considered	Not replaced [33,49,60]
Standby diesel generator	350 $/kW [53]	Not operated	Not replaced [33,47,58]
Diesel engine	289 $/kW [11,46,47,53,58]	5.2 $/kW/a [53]	Not replaced [33,47,58]
MGO tank	1.1$/kgMGO [51,58]	Not considered	Not replaced

The fuel cells are compact containerized solutions that include the stack, its balance of plants, control and monitoring systems, and an integrated DC-DC converter [38]. Their replacement costs are 50% CAPEX because only the degradable components (cells) are replaced periodically when the voltage has dropped by 15% [54]. The rest of the systems (piping, control, monitoring, sensors, vents etc.) inside the stack are non-wearable balance of plant components that are assumed to last 20 years with proper, regular maintenance, without requiring replacement [49]. The process of replacing a degraded stack takes a few hours, so it can take place overnight without the need to take the ship out of service [49].

The batteries require very little maintenance over their lifetime, and the whole rack is replaced after 7 years of operation. They can be operated continuously without requiring to be switched off for extensive maintenance, as required for diesel generators. The rest of the propulsion components of both versions do not require replacement, since with regular maintenance they can last until the end of life of the vessel.

For the fuel cells and the LFP batteries, variable CAPEX has also been considered based on [52,61] respectively, as shown in Fig. 10, to account for CAPEX uncertainty, since these components have low technological maturity levels compared to the rest of the propulsion systems.

The capital cost predictions of fuel cells and batteries are provided until 2029. For the LFP batteries it is assumed that C-rate equals 1. After 2030 (until 2044), it is assumed that the CAPEX remains constant for both components at 600 and 224 $/kW respectively [62].

A sensitivity analysis has been performed for different fuel costs (green hydrogen and MGO), and carbon taxes. In this study, only green

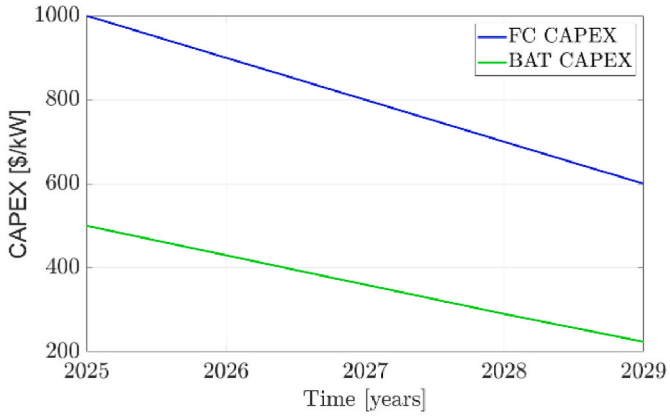

Fig. 10. Variable CAPEX of fuel cells and batteries.

hydrogen has been considered, to minimize the well-to-wake emissions. Four different scenarios, based on literature values, have been considered for its price: a) constant value at 4 $/kg, b) constant value at 6$/kg, c) constant value at 8$/kg, and d) variable fuel cost based on predictions of PwC, from 2025 to 2044 [22,28,63,64]. For MGO, two different scenarios have been considered. Either its price is constant at today's value (0.73 $/kg) for 20 years (averaged from Refs. [47,58,65]), or there is a linear increase over time, as predicted by DNV classification society [46]. The variable fuel price scenarios for green hydrogen and MGO are shown in Fig. 11.

In Fig. 11, the average price over time from the five countries of operation, i.e., Netherlands, Finland, Sweden, Lithuania, and Belgium, has been considered. The Netherlands and Belgium have the lowest green hydrogen prices, and the two Scandinavian countries the highest price over the 20 years. In 2025, it is predicted from PwC [64], that the price of green hydrogen in the Netherlands will be 72% lower than in Finland. This indicates that it might be more cost-effective to refuel hydrogen from either the Netherlands or Belgium, if possible. Considering the low technological maturity of the systems/infrastructure and the potentially limited amount of available green hydrogen, it is recommended to refuel the tank to its limit when there is available quantity at the ports, especially at the early stages of operation, due to the high uncertainty.

Different scenarios have also been considered for carbon tax costs. The implementation of carbon taxes acts as an incentive to reduce emissions by penalising the use of fossil fuels. The implementation of carbon taxes for ships with Gross Tonnage (GT) above 5000 m^3 will start

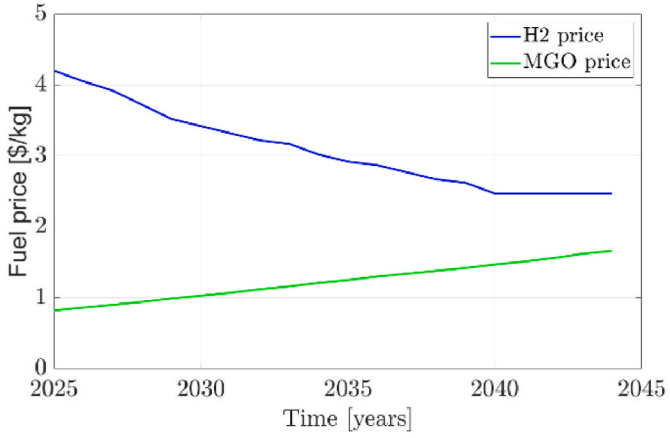

Fig. 11. Variable green hydrogen and MGO prices until 2044. (For interpretation of the references to colour in this figure legend, the reader is referred to the Web version of this article.)

in 2025 based on the European Union Emission Trading System (EU ETS) [66]. The case general cargo vessel sails under a Dutch flag around countries of the EU, and it has a GT less than 5000 m^3. For such ships it is uncertain if and when the carbon taxes will be applied [66,67]. Hence, three different tax cost scenarios have been considered: a) no carbon tax, b) constant carbon tax at 85 $/ton CO_2 over 20 years [66], and c) a variable carbon tax with linear increase, based on PwC predictions [68]. In the last scenario, there is an average carbon tax of 175$/ton CO_2, which can have a significant impact on achieving the maritime decarbonization goals, as stated in Ref. [69]. An emission factor of 3 ton CO_2/ton MGO has been considered in this study based on [32,70].

Hydrogen needs to be liquefied to be stored at the cryogenic tank at the required temperature and pressure conditions. The cost to liquefy hydrogen is assumed to be 1$/kg based on [71]. The transportation cost has not been considered in this study.

The NPV results for the 8 scenarios of the hydrogen-based version, and the 6 scenarios of the diesel-based version are shown in Table 6.

The Fixed CAPEX scenarios are for constant investment costs of all the components, including fuel cells and batteries, over 20 years, based on the prices of 2025. The variable CAPEX scenarios consider the cases that the prices of fuel cells and batteries drop until 2029 and then remain constant (Fig. 10). For the diesel-based version, either a fixed fuel cost is considered (0.73$/kg MGO) or a variable price based on DNV predictions (Fig. 11).

Based on current prices of fuels, components, and carbon taxes (Scenarios 1, 11), the retrofitted hydrogen-based propulsion system has a NPV of $17.62 million, and the original diesel-based version has a NPV of $10.81 million, which is 38.6% less expensive. A more realistic scenario based on the cost predictions and future developments is the following: green hydrogen price declines, MGO prices increases, carbon tax cost increases, CAPEX of fuel cells and batteries decrease (Scenarios 8, 14). As shown in these two scenarios, the NPV of the diesel-based version is 12.8% higher than the hydrogen-based propulsion system, which indicates that the retrofitted version may be more cost-effective from a long-time perspective, if the price trends evolve as expected. In the worst-case scenario of the sensitivity analysis, the NPV of the hydrogen-based version can be up to $18.8 million higher than the original diesel-based system (Scenarios 3, 9), in case hydrogen is not widely used as a fuel in the future.

4.5. Design recommendations and comparison with the diesel-based version

In the hydrogen-based design, there are 9 fuel cells of 150 kW for propulsion, and an additional 10th stack for passive redundancy [72].

Table 6
NPV results for the two versions.

Hydrogen-based version	
Scenarios	Total NPV ($)
1. Fixed CAPEX, 4$/kg	17,624,606
2. Fixed CAPEX, 6$/kg	22,332,508
3. Fixed CAPEX, 8$/kg	27,040,410
4. Fixed CAPEX, PwC H_2 price	15,817,129
5. Variable CAPEX, 4$/kg	17,062,684
6. Variable CAPEX, 6$/kg	21,770,586
7. Variable CAPEX, 8$/kg	26,478,489
8. Variable CAPEX, PwC H_2	15,255,207
Diesel-based version	
Scenarios	Total NPV ($)
9. 0.73$/kg, no carbon tax	8,198,714
10. DNV MGO prices, no tax	12,608,312
11. 0.73$/kg, fixed tax (85$/ton CO_2)	10,815,923
12. DNV MGO prices, fixed tax	15,225,522
13. 0.73$/kg, variable tax (PwC)	13,086,068
14. DNV MGO prices, variable tax	17,495,667

The total battery power and energy of the two racks are 200 kW and 200 kWh respectively. Each power supply component has its DC-DC converter. There are 2 × 710 kW inverters (690V) and 2 × 675 kW induction motors from ABB [73,74]. The main diesel engine from Wartsila [75] in the original configuration can be used as a standby generator, with fewer cylinders, in the new fuel cell-battery propulsion system, as discussed in Section 2.2. The weights and volumes of the main propulsion components of the two versions are shown in Table 7.

The fuel cell stack includes the integrated DC-DC converter and the balance of plant components. The main propulsion system weights and volumes of the two versions are comparable, but the onboard placement of the hydrogen tank (68 tons, 193 m^3) poses significant design and safety challenges, as it will be discussed below in more detail. The total system weight and volume of the hydrogen-based propulsion system is 13,151 kg and 17.16 m^3 respectively, which is only 1.5 tons heavier and occupies around 1.6 m^3 more space than the main engine in the original diesel-based version.

A perspective view of the case vessel is shown in Fig. 12. The accommodation space is below the bridge at the aft of the vessel. The engine room is located right below the accommodation area. It is expected that the propulsion and auxiliary systems of the new hydrogen-based version will fit the existing engine room space (465 m^3), without requiring any change in the dimensions of the vessel, or the cargo carrying capacity. There are five cargo holds ahead of the superstructure. The foredeck is at the bow of the ship.

There are a few possible locations for the LH_2 tank onboard: a) engine room, b) sideways to the bridge, c) in place of one cargo hold at the upper deck, d) foredeck. It is important to note that there should also be an extra margin for the tank connection space, which is usually adjacent to the storage tank, and it contains valves, piping, safety systems, and vaporizers.

Placing the tank below the main deck is not recommended by regulations, since in case of damage, any leakage should not be contained in enclosed spaces, to reduce explosion risks [7,76].

In the existing design (Fig. 12), there is no space at the side of the bridge. Hence, if the tank is to be placed there, the superstructure design should be modified, the tank should be protected from side collisions, the superstructure should be protected from explosions, and ideally the tank should be located more than 20% of the breadth of the vessel from the sides [76]. It is also important to ensure that there is no heat ingress from the accommodation space below the bridge.

Another option is to remove one of the cargo holds and place the tank at its position at the top deck. However, this is not a desired option for shipowners since a certain amount of cargo and thus income is lost. It can also pose a risk in case of crane operation during loading and unloading cargo from adjacent cargo holds.

Placing the tank at the foredeck could also be a possible option if there are no violations of stability criteria. Some other risks that arise are large piping distances and a high number of connecting points that increase the risk of failure and leakage, frontal collision, and reduced visibility from the bridge.

A final option is to change the dimensions of the vessel, but this is not realistic for the 17-year-old case ship. However, it is a design recommendation for similar types of new-built vessels.

Overall, from the design analysis it is shown that retrofitting hydrogen-based ship systems can be challenging in terms of volume, weight and safety due to the large and heavy fuel tank, and the stringent regulatory requirements compared to the diesel setup. In this retrofitting study, the placement of the main propulsion equipment in the existing engine room space did not pose any space or weight issues. However, it is important to follow the safety guidelines of class societies for a detailed design analysis regarding the placement of the equipment in fuel cell and battery rooms. On the other hand, a newbuild ship would be optimized to accommodate the special design and safety requirements of the electrical and fuel systems, without constraints imposed by the existing vessel structure, but at higher CAPEX and lead times compared to a retrofit.

Table 7
Propulsion system weights and volumes.

Systems	Weight (kg)	Volume (m^3)
Fuel cell stacks	3195	5.35
Battery racks	2090	1.58
Inverters	126	0.11
Motors	7740	10.12
Diesel engine	11,600	15.53

Fig. 12. Perspective view of the case vessel.

Fuel cell-battery hybrid systems offer modularity and scalability advantages since they can be used for various ship types (retrofits or newbuilds) and energy demand levels by adjusting the number of the required modules and configurations, depending on the application. The developed model and control strategy can be used for different ship types with similar load profile characteristics, where the battery is used alongside the fuel cell for load smoothing. The same models and controller can also be used for vessels requiring other battery functions such as peak shaving by adjusting the low-pass filter time constant.

5. Conclusions

This study presented a lifetime design, operation, and cost analysis for the propulsion system of a retrofitted cargo vessel with hydrogen fuel cells and batteries. A representative round trip was created by analysing one-year operational data based on the frequency of power distribution and the load ramps. A low-pass filter based real-time controller was employed to distribute the power between the components, by satisfying the energy balance and battery SoC constraint. The batteries were used mainly for ramp support, with an average DoD of 41.3%. The fuel cell degradation was estimated based on a stack voltage degradation model and for the battery degradation, both cycling and calendar aging were considered. The fuel cells require replacement every 5 years, and the batteries every 7 years.

The LH_2 tank (68 tons, 193 m^3) was sized based on the most fuel demanding profile, considering the increased consumption due to component deteriorations, and a 15% spare capacity. Its onboard placement poses significant design and safety challenges, associated with the weight distribution, volume requirements, and explosion risks. The lifetime costs of the energy systems were estimated following a sensitivity analysis with 14 scenarios of varying CAPEX and OPEX. The green hydrogen price and the carbon tax costs had the biggest impact on the NPV value. If the CAPEX and OPEX remain constant over 20 years, the NPV of the retrofitted hydrogen-based version is 38.6% higher than the original diesel-based propulsion system. Based on future predictions that green hydrogen price and fuel cell CAPEX drop, while MGO price

and carbon taxes increase, it is possible that the retrofitted propulsion system can be more cost-effective, from a lifetime perspective, by $ 2.24 million.

CRediT authorship contribution statement

Foivos Mylonopoulos: Writing – original draft, Visualization, Validation, Software, Methodology, Formal analysis, Conceptualization. **Sankarshan Durgaprasad:** Writing – review & editing, Visualization, Validation, Conceptualization. **Andrea Coraddu:** Writing – review & editing, Visualization, Supervision, Methodology, Funding acquisition, Conceptualization. **Henk Polinder:** Writing – review & editing, Visualization, Supervision, Methodology, Funding acquisition, Conceptualization.

Declaration of competing interest

The authors declare that they have no known competing financial interests or personal relationships that could have appeared to influence the work reported in this paper.

Acknowledgments

This research was supported by the Sustainable Hydrogen Integrated Propulsion Drives (SH2IPDRIVE) project, which has received funding from RvO (reference number MOB21013) through the RDM regulation of the Ministry of Economic Affairs and Climate Policy.

References

[1] Khan L, Macklin JJR, Peck BCD, Morton O, Souppez J-BRG. A review of wind-assisted SHIP propulsion for sustainable commercial SHIPping: latest developments and future stakes. Wind Propulsion; 2021. https://doi.org/10.3940/rina.win.2021.05. 2021.
[2] Gritsenko D. Regulating GHG Emissions from shipping: local, global, or polycentric approach? Mar Pol 2017;84:130–3. https://doi.org/10.1016/j.marpol.2017.07.010.
[3] UN. Review of maritime transport 2022. United Nations Conference on Trade and Development; 2022.
[4] IMO. IMO strategy on reduction of GHG emission from ships. International Maritime Organization 2023;4(1). 2023.
[5] Fang S, Wang Y, Gou B, Xu Y. Toward future green maritime transportation: an overview of seaport microgrids and all-electric ships. IEEE Trans Veh Technol 2020;69(1). https://doi.org/10.1109/TVT.2019.2950538.
[6] Inal OB, Charpentier JF, Deniz C. Hybrid power and propulsion systems for ships: current status and future challenges. Renewable and sustainable energy reviews, vol. 156; 2022. https://doi.org/10.1016/j.rser.2021.111965.
[7] Mylonopoulos F, Boulougouris E, Trivyza NL, Priftis A, Cheliotis M, Wang H, Shi G. Hydrogen vs. Batteries: comparative safety assessments for a high-speed passenger ferry. Appl Sci 2022;12(6). https://doi.org/10.3390/app12062919.
[8] Mylonopoulos F, Polinder H, Coraddu A. A comprehensive review of modeling and optimization methods for ship energy systems. IEEE Access 2023;11. https://doi.org/10.1109/ACCESS.2023.3263719.
[9] Ganjian M, Bagherian Farahabadi H, Alirezapouri MA, Rezaei Firuzjaei M. Optimal design strategy for fuel cell-based hybrid power system of all-electric ships. Int J Hydrogen Energy 2024;50. https://doi.org/10.1016/j.ijhydene.2023.07.258.
[10] Vieira GTT, Pereira DF, Taheri SI, Khan KS, Salles MBC, Guerrero JM, Carmo BS. Optimized configuration of diesel engine-fuel cell-battery hybrid power systems in a platform supply vessel to reduce CO2 emissions. Energies 2022;15(6). https://doi.org/10.3390/en15062184.
[11] Wang X, Shipurkar U, Haseltalab A, Polinder H, Claeys F, Negenborn RR. Sizing and control of a hybrid ship propulsion system using multi-objective double-layer optimization. IEEE Access 2021;9:72587–601. https://doi.org/10.1109/ACCESS.2021.3080195.
[12] Wu P, Bucknall R. Hybrid fuel cell and battery propulsion system modelling and multi-objective optimisation for a coastal ferry. Int J Hydrogen Energy 2020;45(4):3193–208. https://doi.org/10.1016/j.ijhydene.2019.11.152.
[13] Bassam AM, Phillips AB, Turnock SR, Wilson PA. An improved energy management strategy for a hybrid fuel cell/battery passenger vessel. Int J Hydrogen Energy 2016;41(47):22453–64. https://doi.org/10.1016/j.ijhydene.2016.08.049.
[14] Bassam AM, Phillips AB, Turnock SR, Wilson PA. Development of a multi-scheme energy management strategy for a hybrid fuel cell driven passenger ship. Int J Hydrogen Energy 2017;42(1):623–35. https://doi.org/10.1016/j.ijhydene.2016.08.209.
[15] Zhu L, Han J, Peng D, Wang T, Tang T, Charpentier JF. Fuzzy logic based energy management strategy for a fuel cell/battery/ultra-capacitor hybrid ship. 2014 1st international conference on green energy, ICGE 2014. 2014. p. 107–12. https://doi.org/10.1109/ICGE.2014.6835406.
[16] Zhao ZH. Improved fuzzy logic control-based energy management strategy for hybrid power system of FC/PV/battery/SC on tourist ship. Int J Hydrogen Energy 2022;47(16):9719–34. https://doi.org/10.1016/j.ijhydene.2022.01.040.
[17] Si Y, Wang R, Zhang S, Zhou W, Lin A, Zeng G. Configuration optimization and energy management of hybrid energy system for marine using quantum computing. Energy 2022;253. https://doi.org/10.1016/j.energy.2022.12413.
[18] Fan F, Aditya V, Xu Y, Cheong B, Gupta AK. Robustly coordinated operation of a ship microgird with hybrid propulsion systems and hydrogen fuel cells. Appl Energy 2022;312. https://doi.org/10.1016/j.apenergy.2022.118738.
[19] Zhu J, Chen L, Wang B, Xia L. Optimal design of a hybrid electric propulsive system for an anchor handling tug supply vessel. Appl Energy 2018;226:423–36. https://doi.org/10.1016/j.apenergy.2018.05.131.
[20] Chen L, Tong Y, Dong Z. Li-ion battery performance degradation modeling for the optimal design and energy management of electrified propulsion systems. Energies 2020;13(7). https://doi.org/10.3390/en13071629.
[21] Wang Z, Li X. Research on multi-objective optimization of capacity allocation for marine hybrid energy storage system. IOP Conf Ser Earth Environ Sci 2021;692(2). https://doi.org/10.1088/1755-1315/692/2/022106.
[22] Bassam AM, Phillips AB, Turnock SR, Wilson PA. Sizing optimization of a fuel cell/battery hybrid system for a domestic ferry using a whole ship system simulator. International conference on electrical systems for aircraft, railway, ship propulsion and road vehicles and international transportation electrification conference, ESARS-ITEC 2016. 2016. https://doi.org/10.1109/ESARS-ITEC.2016.7841333.
[23] Dall'armi C, Pivetta D, Taccani R. Health-conscious optimization of long-term operation for hybrid pemfc ship propulsion systems. Energies 2021;14(13). https://doi.org/10.3390/en14133813.
[24] Dall'Armi C, Pivetta D, Taccani R. Uncertainty analysis of the optimal health-conscious operation of a hybrid PEMFC coastal ferry. Int J Hydrogen Energy 2022;47(21):11428–40. https://doi.org/10.1016/j.ijhydene.2021.10.271.
[25] Zhang Z, Guan C, Liu Z. Real-time optimization energy management strategy for fuel cell hybrid ships considering power sources degradation. IEEE Access 2020;8:87046–59. https://doi.org/10.1109/ACCESS.2020.2991519.
[26] Chen H, Zhang Z, Guan C, Gao H. Optimization of sizing and frequency control in battery/supercapacitor hybrid energy storage system for fuel cell ship. Energy 2020;197. https://doi.org/10.1016/j.energy.2020.117285.
[27] Lagemann B, Lindstad E, Fagerholt K, Rialland A, Ove Erikstad S. Optimal ship lifetime fuel and power system selection. Transport Res Transport Environ 2022;102. https://doi.org/10.1016/j.trd.2021.103145.
[28] Lagemann B, Lagouvardou S, Lindstad E, Fagerholt K, Psaraftis HN, Erikstad SO. Optimal ship lifetime fuel and power system selection under uncertainty. Transport Res Transport Environ 2023;119. https://doi.org/10.1016/j.trd.2023.103748.
[29] Al-Falahi MDA, Coleiro J, Jayasinghe SDG, Enshaei H, Garaniya V, Baguley C, Madawala U. Techno-economic feasibility study of battery- powered ferries. 2018 IEEE 4th southern power electronics conference, SPEC 2018. 2018. https://doi.org/10.1109/SPEC.2018.8636010.
[30] Wang H, Aung MZ, Xu X, Boulougouris E. Life cycle analysis of hydrogen powered marine vessels—case ship comparison study with conventional power system. Sustainability 2023;15(17). https://doi.org/10.3390/su151712946.
[31] Inal OB, Zincir B, Dere C, Charpentier J-F. Hydrogen fuel cell as an electric generator: a case study for a general cargo ship. J Mar Sci Eng 2024;12:432. https://doi.org/10.3390/jmse12030432.
[32] Karvounis P, Theotokatos G, Boulougouris E. Environmental-economic sustainability of hydrogen and ammonia fuels for short sea shipping operations. Int J Hydrogen Energy 2024;57:1070–80. https://doi.org/10.1016/j.ijhydene.2024.01.058.
[33] Trillos JCG, Wilken D, Brand U, Vogt T. Life cycle assessment of a hydrogen and fuel cell ropax ferry prototype. In: Sustainable production, life cycle engineering and management; 2021. https://doi.org/10.1007/978-3-030-50519-6_2.
[34] Mylonopoulos F, Kopka T, Coraddu A, Polinder H. A model-based parametric study for comparison of system configurations and control of a hydrogen hybrid cargo vessel. Modelling and Optimisation of Ship Energy Systems 2023;2023. https://doi.org/10.59490/moses.2023.671.
[35] Ma N, Zhao W, Wang W, Li X, Zhou H. Large scale of green hydrogen storage: opportunities and challenges. Int J Hydrogen Energy 2024;50. https://doi.org/10.1016/j.ijhydene.2023.09.021.
[36] Hasturk U, Schrotenboer AH, Ursavas E, Roodbergen KJ. Stochastic cyclic inventory routing with supply uncertainty: a case in green-hydrogen logistics. Transport Sci 2024;58(2). https://doi.org/10.1287/trsc.2022.0435.
[37] Allan DA, Bates CN, Risbeck MJ, Rawlings JB. On the inherent robustness of optimal and suboptimal nonlinear MPC. Syst Control Lett 2017;106. https://doi.org/10.1016/j.sysconle.2017.03.005.
[38] Maritime hydrogen fuel cell systems - zepp.Solutions. Retrieved February 1, 2024, from https://zepp.solutions/en/maritime-fuel-cell-systems/.
[39] Lorenzo C, Bouquain D, Hibon S, Hissel D. Synthesis of degradation mechanisms and of their impacts on degradation rates on proton-exchange membrane fuel cells and lithium-ion nickel–manganese–cobalt batteries in hybrid transport applications. Reliability engineering and system safety, vol. 212; 2021. https://doi.org/10.1016/j.ress.2020.107369.
[40] Reddy NP, Skjetne R, Os OS, Papageorgiou D. A comparison of the state-of-the-art reinforcement learning algorithms for health-aware energy & emissions management in zero-emission ships. IEEE Journal of Emerging and Selected Topics in Industrial Electronics 2024;5(1). https://doi.org/10.1109/JESTIE.2023.3331230.

[41] Feng Y, Dong Z. Integrated design and control optimization of fuel cell hybrid mining truck with minimized lifecycle cost. Appl Energy 2020;270. https://doi.org/10.1016/j.apenergy.2020.115164.
[42] Fletcher T, Thring R, Watkinson M. An Energy Management Strategy to concurrently optimise fuel consumption & PEM fuel cell lifetime in a hybrid vehicle. Int J Hydrogen Energy 2016;41(46). https://doi.org/10.1016/j.ijhydene.2016.08.157.
[43] Schaltz E, Khaligh A, Rasmussen PO. Influence of battery/ultracapacitor energy-storage sizing on battery lifetime in a fuel cell hybrid electric vehicle. IEEE Trans Veh Technol 2009;58(8).
[44] GreenBattery - Praxis Automation Technology B.V. Retrieved, https://www.praxis-automation.eu/products/electric-energy-storage/; 2024.
[45] Ali H, Beltran H, Lindsey NJ, Pecht M. Assessment of the calendar aging of lithium-ion batteries for a long-term—space missions. Front Energy Res 2023;11. https://doi.org/10.3389/fenrg.2023.1108269.
[46] Soni G, Neto RC, Moreira L. Hydrodynamic simulation of green hydrogen catamaran operating in Lisbon, Portugal. J Mar Sci Eng 2023;11:2273. https://doi.org/10.3390/jmse11122273.
[47] Perčić M, Vladimir N, Jovanović I, Koričan M. Application of fuel cells with zero-carbon fuels in short-sea shipping. Appl Energy 2022;309. https://doi.org/10.1016/j.apenergy.2021.118463.
[48] Pratt JW, Klebanoff LE. Feasibility of SF-BREEZE: a zero emission hydrogen fuel cell high speed passenger ferry. Sandia Report, Sandia National Laboratories; 2016.
[49] Aarskog FG, Danebergs J, Strømgren T, Ulleberg Ø. Energy and cost analysis of a hydrogen driven high speed passenger ferry. Int Shipbuild Prog 2020;67(1). https://doi.org/10.3233/ISP-190273.
[50] Cichowicz J, Theotokatos G, Vassalos D. Dynamic energy modelling for ship life-cycle performance assessment. Ocean Eng 2015;110. https://doi.org/10.1016/j.oceaneng.2015.05.041.
[51] TNO. Tno power-2-fuel cost analysis - smartport. Retrieved from: https://smartport.nl/wp-content/uploads/2020/09/CostAnalysis-Power-2-Fuel_def_2020.pdf; 2020.
[52] Fueling the Future of Mobility: hydrogen and fuel cell solutions for transportation. Retrieved from: deloitte-cn-fueling-the-future-of-mobility-en-200101.pdf.
[53] Kim K, Roh G, Kim W, Chun K. A preliminary study on an alternative ship propulsion system fueled by ammonia: environmental and economic assessments. J Mar Sci Eng 2020;8(3). https://doi.org/10.3390/jmse8030183.
[54] Thomas D. Cost reduction potential for electrolyser technology; hydrogenics. Mississauga, ON, Canada; 2018.
[55] Chen X, Long S, He L, Wang C, Chai F, Kong X, Wan Z, Song X, Tu Z. Performance evaluation on thermodynamics-economy-environment of PEMFC vehicle power system under dynamic condition. Energy Convers Manag 2022;269.
[56] Cigolotti V, Genovese M, Fragiacomo P. Comprehensive review on fuel cell technology for stationary applications as sustainable and efficient poly-generation energy systems. Energies 2021;14(16). https://doi.org/10.3390/en14164963.
[57] Vieira GTT, Pereira DF, Taheri SI, Khan KS, Salles MBC, Guerrero JM, Carmo BS. Optimized configuration of diesel engine-fuel cell-battery hybrid power systems in a platform supply vessel to reduce CO2 emissions. Energies 2022;15(6). https://doi.org/10.3390/en15062184.
[58] Kistner L, Bensmann A, Hanke-Rauschenbach R. Potentials and limitations of battery-electric container ship propulsion systems. Energy Convers Manag X 2024;21. https://doi.org/10.1016/j.ecmx.2023.100507.
[59] Shin HK, Ha SK. A review on the cost analysis of hydrogen gas storage tanks for fuel cell vehicles. Energies 2023;16(13). https://doi.org/10.3390/en16135233.
[60] Derking H, van der Togt L, Keezer M. Liquid hydrogen storage: status and future perspectives. Cryoworld BV; 2019.
[61] Battery storage and renewables: costs and markets to 2030. Retrieved March 1, 2024, from https://www.irena.org/publications/2017/Oct/Electricity-storage-and-renewables-costs-and-markets.
[62] Edelenbosch OY, Hof AF, Nykvist B, Girod B, van Vuuren DP. Transport electrification: the effect of recent battery cost reduction on future emission scenarios. Climatic Change 2018;151(2). https://doi.org/10.1007/s10584-018-2250-y.
[63] Chen H, Pei P, Song M. Lifetime prediction and the economic lifetime of proton exchange membrane fuel cells. Appl Energy 2015;142. https://doi.org/10.1016/j.apenergy.2014.12.062.
[64] Green hydrogen economy - predicted development of tomorrow: PwC. Retrieved March 1, 2024,from https://www.pwc.com/gx/en/industries/energy-utilities-resources/future-energy/green-hydrogen-cost.html.
[65] Rotterdam Bunker Prices - Ship & Bunker. Retrieved March 1, 2024, from https://shipandbunker.com/prices/emea/nwe/nl-rtm-rotterdam.
[66] EU ETS — Sustainable Ships. Retrieved March 1, 2024, from https://www.sustainable-ships.org/rules-regulations/eu-ets.
[67] FAQ – Maritime transport in EU Emissions Trading System (ETS) - European Commission. Retrieved March 1, 2024, from https://climate.ec.europa.eu/eu-action/transport/reducing-emissions-shipping-sector/faq-maritime-transport-eu-emissions-trading-system-ets_en.
[68] Energy transition: CO2 levy & NL CO2 tax (In Dutch) - State of Tax - Events - PwC. Retrieved March 1,2024,from https://www.pwc.nl/en/services/tax/webcast-series-state-of-tax/energy-transition.html.
[69] Getting to Zero Coalition. Policy options for closing the competitiveness gap between fossil and zero-emission fuels in shipping. https://www.globalmaritimeforum.org/content/2021/11/INSIGH1.pdf; 2021.
[70] Karagiorgis S, Nasiri S, Polinder H. Implementation of ship hybridisation: sizing a hybrid crew transfer vessel considering uncertainties. Proceedings of the international naval engineering conference, vol. 2022; 2022.
[71] al Ghafri SZ, Munro S, Cardella U, Funke T, Notardonato W, Trusler, et al. Hydrogen liquefaction: a review of the fundamental physics, engineering practice and future opportunities. Energy Environ Sci 2022;15(7). https://doi.org/10.1039/d2ee00099g.
[72] Balestra L, Schjølberg I. Modelling and simulation of a zero-emission hybrid power plant for a domestic ferry. Int J Hydrogen Energy 2021;46(18):10924–38. https://doi.org/10.1016/j.ijhydene.2020.12.187.
[73] ACS880 drive modules - Optimized for cabinet assembly - Industrial drives - Uncompromised productivity (Low voltage AC) | ABB. Retrieved March 1, 2024, from https://new.abb.com/drives/low-voltage-ac/industrial-drives/acs880-drive-modules.
[74] AXR 400ML6 680 KW 4160V ABB high voltage induction motors 1193 rpm 60HZ. Retrieved February 25, 2024, from https://motors.bonnew.com/axr-400ml6-680kw-4160v-60hz.html.
[75] Wärtsilä 20 - Diesel engine. Retrieved March 1,2024,from https://www.wartsila.com/marine/products/engines-and-generating-sets/diesel-engines/wartsila-20.
[76] Wang H, Trivyza NL, Mylonopoulos F, Boulougouris E. Comparison of decarbonisation solutions for shipping: hydrogen, ammonia and batteries. SNAME 14th international marine design conference, IMDC 2022. 2022.